Aalborg Universitet

AALBORG UNIVERSITY

DENMARK

Charge States of Size-Selected Silver Nanoparticles Produced by Magnetron Sputtering

Popok, Vladimir; Gurevich, Leonid

Publication date:
2019

Document Version
Accepted author manuscript, peer reviewed version

Link to publication from Aalborg University

Charge States of Size-Selected Silver Nanoparticles Produced by Magnetron Sputtering

Vladimir N. Popok · Leonid Gurevich

Abstract

Gas-phase aggregation of metal nanoparticles (nanoclusters), in particular using magnetron sputtering, is a widely used method in research and industrial applications. Therefore, better understanding of the nucleation and growth processes as well as of nanoparticle dynamics in aggregation zone is required. One of the poorly understood issues is a charge state of nanocluster formed in magnetron-based sources. In the current work, an original approach to study charge states of silver nanoclusters after mass (size) filtering is suggested. The study reveals that particles can carry both negative and positive charges; anionic nanoparticles dominate over the cationic ones. It is also found that a considerable fraction of nanoparticles has charges greater than unity and this fraction increases with particle size. However, the tendency depends on polarity. For the cations, the doubly-, triply- and quadruply-charged NCs have very similar fractions for a given filtering condition, while for anions, an ability to carry higher than unity charges by individual particles gradually decreases. Thus, the study provides important insights on the formation of cationic and anionic nanoparticles in magnetron cluster sources as well as on the tendencies to carry multiple charges depending on particle size.

Keywords: gas aggregated metal nanoparticles, cluster beam technique, cluster size selection, charge state of nanoparticle

Vladimir N. Popok (vp@mp.aau.dk) · Leonid Gurevich

Department of Materials and Production, Aalborg University, Skjernvej 4A, 9220 Aalborg, Denmark

Introduction

Gas-phase aggregation of metal nanoparticles (NPs) is one of the attractive applied methods used in nanoscience and nanotechnology. Atomic vapour can be produced by heating or sputtering of a target. And then, creating conditions for supersaturation causes nucleation and growth of nanoclusters (NC, aggregates of atoms) (Haberland 1994, Binns 2001). Among different approaches for sputtering, magnetron systems were found to be very efficient and easy in use for NP formation. In the pioneering work by Haberland et al. 1991, metal target installed in a vacuum chamber was sputtered using Ar^+ ions created by magnetron discharge. The metal vapour was swept into a condensation cell where conditions facilitating nucleation and growth of NCs were maintained. The NPs expanded from the cell were collimated into a beam by skimmer and transferred into the next chamber for further characterisation or deposition (Haberland et al. 1992). Since then, this technique underwent a number of improvements and was developed into commercial magnetron-based cluster sources, becoming more and more popular as witnessed by the increasing number of publications.

In the recent years, these sources have been widely used for the formation of NPs of various metals, alloys and compounds as well as core-shell structures. For an overview of the technique and its capabilities one can refer to Huttel (ed) 2017, Polonskyi et al. 2018, Liamosa et al. 2014 and references therein. Adding size-selection (mass-filtering) setups (Binns 2001, Popok 2009) to the magnetron-based aggregation sources allows choosing NPs of particular masses out of an entire range of sizes varying from a few tens to millions of atoms. For instance, a time-of-flight mass filter brings a capability to obtain a constant mass resolution ($M/\Delta M \sim 25$) in a wide size range while keeping NC beam intensity reasonably high (Pratontep et al. 2005). Use of an electrostatic quadrupole mass selection (EQMS) allows to filter NPs with precision ±10% of particle size (Hartmann et al 2012,

Hanif et al. 2016). An advantage of this filtering approach is a possibility to choose between positively and negatively charged clusters.

Thus, formation of NPs using magnetron sputtering and gas aggregation is a powerful and versatile approach bringing a number of practical benefits. Therefore, there have been continuous efforts on further improvement of the technique, in particular through better understanding of NC nucleation and growth processes as well as dynamics of NPs in the aggregation zone. It is shown that the buffer gas pressure, flow rate and temperature are essential parameters affecting cluster sizes (Polonskyi et al. 2018). It has also been found, e.g., for Cu and Ag that the majority of NCs and also the heaviest of them become trapped in the near-to-magnetron cloud (Kousal et al. 2018, Nikitin et al. 2019) while only some fraction of lighter particles can escape and be transferred to next chamber for following use. This trapping is explained by the influence of magnetron electro-magnetic field on charged NCs.

Metal NPs produced in magnetron-based sources can carry both positive and negative charges (Momin and Bhowmick 2010, Ganeva et al. 2013). The ratio of cations and anions is found to depend on sputtering conditions, in particular, on plasma density (Ahadi et al. 2016). It is also proposed that NCs obtained by magnetron sputtering can carry a multiple charge. For instance, this assumption is used to explain the so-called "planetary" silver NP systems found after magnetron sputtering (Marom et al. 2019). These "planetary" assemblies consist of a large particle surrounded by a few small satellites, which are held in orbits by a balance of the Coulomb and centrifugal forces. The model is based on a possibility to carry charges higher than unity by NPs in order to achieve stability of the systems. However, to our best knowledge the issue of multiple NC charge states has not been experimentally studied so far while it is of theoretical importance for the cluster formation process in the magnetron sputtering sources and of practical significance for the production of metal NPs with desired properties. In particular, charge states are essential for NP deposition on surfaces

functionalized with either positive or negative net charges. For example, negatively charged Ag NCs were coupled to positively charged amine groups formed on quartz surface, thus, promoting formation of reliable optical transducers for biosening (Fojan et al. 2015). Modulation of electrostatic potential in polymeric grooves produced with nanoscale lithography allowed to push limits in precise positioning of NPs and achieve formation of 1D NP arrays (Chen et al. 2017). Use of NCs with controlled charge state could further facilitate this method.

In this work, we suggest an original approach for evaluation of the charge states of silver particles produced by magnetron sputtering cluster apparatus (MaSCA) and filtered by EQMS. Silver nanostructures are of a high interest for numerous applications in plasmonics and sensing (Scholl et al. 2012, Jeon et al. 2016, Novikov et al. 2017).

Experimental

Silver NPs were produced using a commercial nanocluster source (NC200U from Oxford Applied Research) attached to home-built vacuum system, which together with the source, was called MaSCA. A schematic drawing of the apparatus is shown in Fig. 1. Main parts of the system were earlier described elsewhere (Hanif et al. 2015, Popok et al. 2017). In the current configuration, an Einzel lens was added between EQMS and Deposition chamber allowing to control a beam diameter when depositing NCs on a substrate. A silver target of 99.99% purity in a shape of disk with diameter of 50 mm was used for NC formation. The source was operated in DC regime at a power of 64-66 W. Ar with flows of 63-65 sccm was utilized for sputtering and He with flows of 30-35 sccm for promoting NC aggregation. Walls of the aggregation chamber were cooled with liquid nitrogen typically to the temperatures between $-20 \div -25\ ^oC$. Background pressure in the source chamber (after the nozzle) was $4\text{-}5 \times 10^{-8}$ mbar, which was increased to $2\text{-}3 \times 10^{-3}$ mbar under the magnetron operation.

Background pressure in the deposition chamber was kept at 3×10^{-7} mbar (increased to $5\text{-}6 \times 10^{-6}$ mbar during the cluster beam deposition).

EQMS is one of the key elements for the current study. Details of the configuration and construction can be found elsewhere (Hartmann et al. 2012). The operation principle is based on deflection of charged particles in an electric field with hyperbolical equipotential lines (Denison 1971 and Zeman 1977). At a given electrostatic potential U applied to the electrodes, the particle pass energy E through the mass selector is defined by simple equation

$$E = kqU, \tag{1}$$

where q is the particle charge and k is the correction coefficient related to real shape of electrodes and their mutual positions causing deviations from ideal hyperbolic geometry. This equation defines conditions for cluster deflection exactly for 90° inside EQMS and, thus, transferring these NCs into the deposition chamber (see Fig. 1). The above-mentioned pass energy is the cluster kinetic energy $E = mv^2/2$. Assuming that all NCs entering the EQMS have the same velocity, eq. (1) can be rearranged as following

$$\frac{m}{q} \sim U, \tag{2}$$

where m is the NC mass. Eq. (2) tells us that for a given potential applied to the electrodes only the particles of a certain mass-to-charge ratio will pass the filtering and become deposited on a substrate. If NC has a unit charge, filtering provides a certain mass m. However, if the charge is equal to 2 or 3, then, respectively, the particles with double and triple masses will be selected under the same applied potential. Recent studies of silver NPs size-selected and deposited using MaSCA (Novikov et al. 2017) showed that they preserve nearly spherical shape due to the soft-landing regime (Popok 2009). Thus, the particles of double or triple mass will correspond to spheres with diameters factor of $\sqrt[3]{2}$

and $\sqrt[3]{3}$ larger, respectively. Change of polarity applied to pairs of electrodes (see Fig. 1) allows switching between deflection of either positively or negatively charged (cationic and anionic, respectively) NCs.

This brings us to the idea of current experiment. Silver NPs selected under given EQMS potentials of 200, 500 and 1100 V were deposited on Si substrates with low roughness (RMS = 0.15-0.20 nm for 2x2 μm^2). Height distributions of these NPs were obtained by atomic force microscopy (AFM) using Ntegra Aura system (from NT-MDT). The areas of 2x2 μm^2 were scanned with resolution of 512x512 in tapping mode by commercial ultra-sharp silicon cantilevers. The obtained histograms were fitted with a sum of Gaussians centred at h (the most abundant height), $\sqrt[3]{2}h, \sqrt[3]{3}h$ etc., hence, allowing to distinguish singly-, doubly-, triply- etc. charged NPs. The experiments were carried out under the different polarities applied to EQMS electrodes, thus, allowing to deposit either cationic or anionic NCs for the same potential value. For every used EQMS potential and polarity, two samples were prepared and 2-3 areas were scanned by AFM on every sample. This approach allowed us to obtain sufficient statistics for analysis: between 700 and 2500 NPs for every deposition condition.

Results and Discussion

Examples of AFM images used for the analysis are shown in Fig. 2. They represent the samples with deposited positively-charged Ag NCs selected at 200 V and with negatively-charged ones selected at 1100 V. Areas with cluster aggregated after the deposition or with some suspicious features were excluded from the height analysis. Some of such areas are show in Fig. 2 by circles.

Histograms of NCs selected at 200 V are given in Fig. 3. It is worth noting that these and all following histograms include data from several AFM scans. It is seen in Fig. 3(a) that along with the

most abundant $h = 7.5$ nm, two more Gaussian distributions corresponding to 9.4 ($\sqrt[3]{2}h$) and 10.8 nm ($\sqrt[3]{3}h$) are present, thus evidencing NCs with higher charges for negative polarity. Similar fits are shown in Fig. 3(b) representing the same most abundant h but for positively charged NCs. Interestingly, the fraction of multiply-charged NCs is found to be lower for the cations than for anions. More details on the fractions of NCs with different charges are given in Table 1.

With increasing filtering potential, particle size increases too. For 500 V, the best fit of the height distributions is achieved with four Gaussians (see Fig. 4). The most abundant heights corresponding to singly- and multiply-charged NPs are found to have close values for negative and positive polarities; within expected standard deviation of 10%. Similar to the case of 200 V, the multiply-charged NCs dominate for negative polarity; their total fraction is about 0.16. Among those, the doubly-charged particles prevail (fraction is 0.11), while the fraction of triply-charged ones is very small (0.04) and quadruply-charged NPs are only present in tiny amounts (0.01). On the other hand, for the positively charged NPs, the fraction of those missing only one electron is still high, 0.92, and it is about the same as for 200 V, 0.90 (see Tab. 1). It is worth noting that doubly-, triply- and quadruply-charged NPs are present in more or less equal fractions of 0.02-0.03.

Under further increase of particle size (filtering potential of 1100 V), the probability to carry higher charges rises for both anions and cations; fraction of singly-charged particles is reduced to 0.72-0.79 (see Fig. 5 and Tab. 1). For the case of negative polarity, the NCs carrying double charge prevail among those with triple or quadruple ones. On the other hand, for the positive polarity, the doubly-, triply- and quadruply-charged NPs are found in smaller but almost equal fractions (see Tab. 1) meaning that probabilities of losing 2, 3 or 4 electrons are very similar for silver NCs.

Thus, we can summarise on the following observed tendencies. In our experiments on the silver cluster beams produced by magnetron sputtering, particles with negative polarity dominate over those

with positive one. For the silver NPs of same size, there is a higher probability to catch extra electrons than to lose them. This tendency is not very clear. According to theoretical simulations, one can obtain both the stable silver cations and anions (Häkkinen et al. 2004, Blom et al. 2006, Yang et al. 2007, McKee et al. 2017). However, due to the limitations of computational power the modelling can be performed only for relatively small NCs comprised of less than 200 atoms. In our case, the spherical cluster approximation suggests that our smallest NPs with mean diameter of 7.4 nm consist of ca. 11000 atoms, while those with diameter of 25.2 nm are of approximately 445000 atoms. Particles of such sizes are known to follow bulk-like FCC structure (Hartmann et al 2012, Novikov et al. 2017) forming polyhedrons, which can be predicted by simple Wulff constructions (Carchini et al. 2013). Thus, charge states of such large NPs can be treated by considering atoms located in surface crystalline facets and in low-coordinated sites (steps, edges and corners).

It is found that fraction of multiply-charged NCs in the beam increases with size, i.e. number of atoms comprising the particles. However, the tendencies are different for negative and positive polarities. For the cations and given filtering condition (potential), we observe very similar fractions of the doubly-, triply- and quadruply-charged NCs. It is known that generally silver has tendency to donate electrons. Thus, it should be energetically favourable to have cations in the cluster surface positions with low coordination numbers. For the anions, fraction of multiply-charged NCs in the beam decreases gradually, i.e. the doubly-charged NCs dominate over triply-charged ones and the latter prevail over the quadruply-charged NCs. Presence of an extra electron on an individual atom would increase its energy and should lead to high probability for separation of this atom from the NP. Thus, one can suggest that extra electon(s) is/are delocalised among the surface atoms of NCs. With increasing particle size, number of surface atoms is also increased allowing to allocate more extra electrons on a single NP. This hypothesis explains well the experimental observations showing an increased fraction of multiply-charged anionic NCs.

Conclusion

In the current paper, a methodology for distinguishing between singly- and multiply-charged NCs produced by magnetron-based gas-phase aggregation, mass-filtered in electrostatic field and deposited on a flat substrate, is suggested. Assuming that the NPs preserve spherical (or almost spherical) shape under soft-landing, i.e. the height of a NP measured by AFM is equal to its diameter, one can relate the obtained height distributions to the charge states of NPs. The proposed method is tested using silver NPs selected at 3 different electrostatic potentials with both positive and negative polarity for every case.

It is found that silver NCs can carry both positive and negative charges higher than unity. Under the sputtering and aggregation conditions used in the current experiments, anionic NPs dominate over the cationic ones in the silver cluster beam. Cationic NCs typically have a lower fraction of multiply-charged NPs compared to the anionic ones of the same size. The fraction of multiply-charged NCs increases with particle size. However, the tendency depends on polarity. For the cations, the doubly-, triply- and quadruply-charged NCs have very similar fractions for a given filtering condition. This finding can be explained by transition of atoms located in low-coordinated surface sites into a cationic state, which should be energetically favourable. For anions, fractions of multiply-charged NPs gradually decrease with increasing charge. It is suggested that extra electrons are delocalised over a number of surface atoms and, therefore, probabilities to allocate higher number of electrons on a cluster are low for NPs of small sizes, while increase with particle diameter.

One more important practical conclusion of the carried out research is that EQMS provides relatively good filtering only for small (less massive) silver NPs. With increasing size (mass), the mass filtering becomes worth due to a larger fraction of multiply-charged NCs.

Conflict of Interest The authors declare that they have no conflict of interest.

References

Bins C (2001) Nanoclusters deposited on surfaces. Surf Sci Rep 44: 1-49.

Blom MN, Schooss D, Stairs J, Kappes MM (2006) Experimental structure determination of silver cluster ions (Ag_n^+, $19 \leq n \leq 79$). J Chem Phys 124: 244308.

Carchini G, Almora N, Revilla-Lopez G, Bellarosa L, García-Muelas R, García Melchor M, Pogodin S, Błonski P, Nuria López N (2013) How theoretical simulations can address the structure and activity of nanoparticles. Top Catal 56: 1262-1272.

Chen J, Huang J, Toma A, Zhong L, Cui Z, Shao W, Li Z, Liang W, De Angelis F, Jiang L, Chi L (2017) Modulating the spatial electrostatic potential for 1D colloidal nanoparticles assembly. Adv Mater Interfaces 4: 1700505.

Denison DR (1971) Operating Parameters of a Quadrupole in a Grounded Cylindrical Housing. J Vac Sci Technol 8: 266-269.

Fojan P, Hanif M, Bartling S, Hartmann H, Barke I, Popok VN (2015) Supported silver clusters as nanoplasmonic transducers for protein sensing. Sensors Actuators B 212: 377-381.

Ganeva M, Pipa AV, Smirnov, BM, Kashtanov PV, Hippler R (2013) Velocity distribution of mass-selected nano-size cluster ions. Plasma Sources Sci Technol 22: 045011.

Haberland H, Karrais M, Mall M (1991) A new type of cluster and cluster ion source. Z Phys D 20: 413-415.

Haberland H, Karrais M, Mall M,Thurner Y (1992) Thin films from energetic cluster impact: a feasibility study. J Vac Sci Technol A 10: 3266-3271.

Haberland H (1994) Experimental methods. In: Haberland H (ed) Clusters of atoms and molecules. Springer-Verlag, Berlin, pp 205-252.

Hanif M, Juluri RR, Chirumamilla M, Popok VN (2016) Poly (methyl methacrylate) Composites with Size-Selected Silver Nanoparticles Fabricated using Cluster Beam Technique. J Polym Sci B: Polym Phys 54: 1152-1159.

Hartmann H, Popok VN, Barke I, von Oeynhausen V, Meiwes-Broer K-H (2012) Design and capabilities of an experimental setup based on magnetron sputtering for formation and deposition of size-selected metal clusters on ultra-clean surfaces. Rev Sci Instrum 83: 073304.

Huttel Y (ed) (2017) Gas-phase synthesis of nanoparticles. Wiley-VCH, Weinheim.

Häkkinen H, Moseler M, Kostko O, Morgner N, Hoffmann M A, von Issendorff B (2004) Symmetry and electronic structure of noble-metal nanoparticles and the role of relativity. Phys. Rev. Lett. 93: 093401.

Jeon TY, Kim DJ, Park S-G, Kim S-H, Kim D-H (2016) Nanostructured plasmonic substrates for use as SERS sensors. Nano Convergence 3: 18.

Kousal J, Shelemin A, Schwartzkopf M, Polonskyi O, Hanus J, Solar P, Vaidulych M, Nikitin D, Pleskunov P, Krtous Z, Stunskus T, Faupel F, Roth SV, Biederman H, Choukourov A (2018) Magnetron-sputtered copper nanoparticles: lost in gas aggregation and found by in situ X-ray scattering. Nanoscale 10: 18275.

Liamosa D, Ruano M, Martinez L, Mayoral A, Roman E, Garcia-Hernandez M, Huttel Y (2014) The ultimate step towards a tailored engineering of core@shell and core@shell@shell nanoparticles. Nanoscale 6: 13483-13486.

Marom S, Plesser M, Modi R, Manini N, Di Vice M (2019) 'Planetary' silver nanoparticles originating from a magnetron sputter plasma. J Phys D: Appl Phys 52: 095301.

McKee ML, Samokhvalov A (2017) Density Functional Study of Neutral and Charged Silver Clusters Ag_n with n=2−22. Evolution of Properties and Structure. J Phys Chem A 121: 5018-5028.

Momin T, Bhowmick A (2010) A new magnetron based gas aggregationsource of metal nanoclusters coupled to adouble time-of-flight mass spectrometer system. Rev Sci Instr 81: 075110.

Nikitin D, Hanuš J, Ali-Ogly S, Polonskyi O, Drewes J, Faupel F, Biederman H, Choukourov A (2019) The evolution of Ag nanoparticles inside a gas aggregation cluster source. Plasma Proc Polym in press.

Novikov SM, Popok VN, Evlyukhin AB, Hanif M, Morgen P, Fiutowski J, Beermann J, Rubahn H-G, Bozhevolnyi SI (2017) Highly-stable monocrystalline silver clusters for plasmonic applications. Langmuir 33: 6062-6070.

Polonskyi O, Ahadi AM, Peter T, Fujioka K, Abraham JW, Vasiliauskaite E, Hinz A, Strunskus T, Wolf S, Bonitz M, Kersten H, Faupel F (2018) Plasma based formation and deposition of metal and metal oxide nanoparticles using a gas aggregation source. Eur Phys J D 72: 93.

Popok V (2009) Energetic cluster-surface collisions. In: Sattler KD (ed) Handbook of nanophysics, V 2, Clusters and fullerenes. CRC Press, Boca Raton, pp 19-1–19-19.

Popok VN, Hanif M, Ceynowa FA, Fojan P (2017) Immersion of low-energy deposited metal clusters into poly(methyl methacrylate). Nucl Instrum Meth Phys Res B 409: 91-95.

Pratontep S, Carrol Sj, Xirouchaki C, Streun M, Palmer RE (2005) Size-selected cluster beam source based on radio frequency magnetron plasma sputtering and gas condensation. Rev Sci Instrum 76: 045103.

Scholl JA, Koh AL, Dionne JA (2012) Quantum plasmon resonances of individual metallic nanoparticles. Nature 483: 421-427.

Yang X, Cai W, Shao X. (2007) Structural Variation of Silver Clusters from Ag_{13} to Ag_{160}. J Phys Chem A 111: 5048−5056.

Zeman HD (1977) Deflection of an ion beam in the two-dimensional electrostatic quadrupole field. Rev Sci Instrum 48: 1079-1085.

Table 1. Most abundant heights measured by AFM and fractions of singly- and multiply-charged NCs filtered at different potentials and polarities.

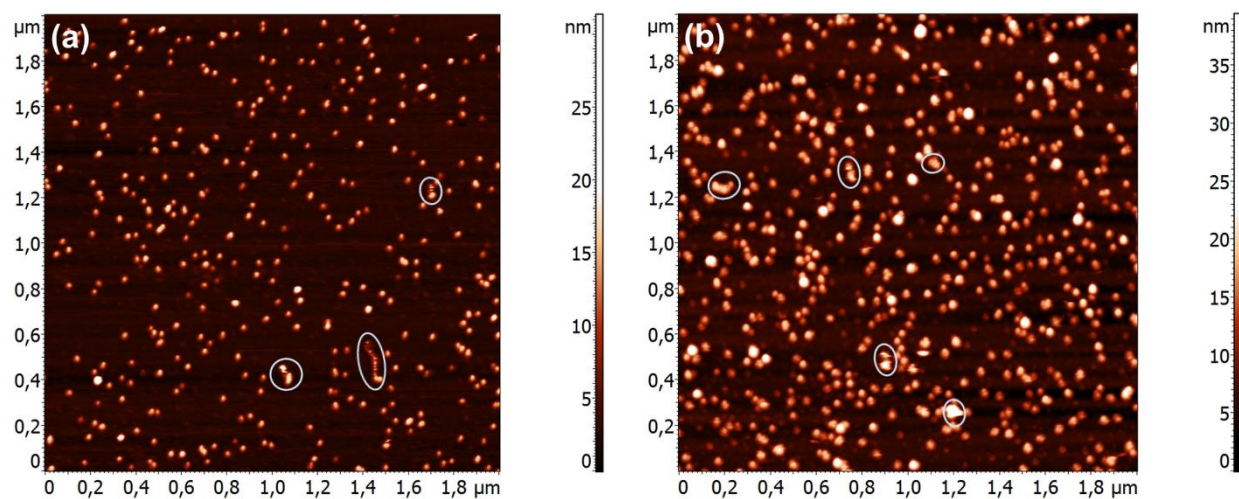| Potential (V), Polarity	Most abundant height (nm)/Fraction			
	Singly-charged	Doubly-charged	Triply-charged	Quadruply-charged
200, "–"	7.5/0.82	9.4/0.11	10.8/0.07	–
200, "+"	7.4/0.90	9.4/0.06	10.7/0.04	–
500, "–"	11.4/0.84	14.4/0.11	16.5/0.04	18.2/0.01
500, "+"	10.8/0.92	13.6/0.03	15.6/0.02	17.2/0.03
1100, "–"	14.7/0.72	18.5/0.15	21.2/0.07	23.3/0.06
1100,"+"	15.9/0.79	20.0/0.07	22.9/0.06	25.2/0.08
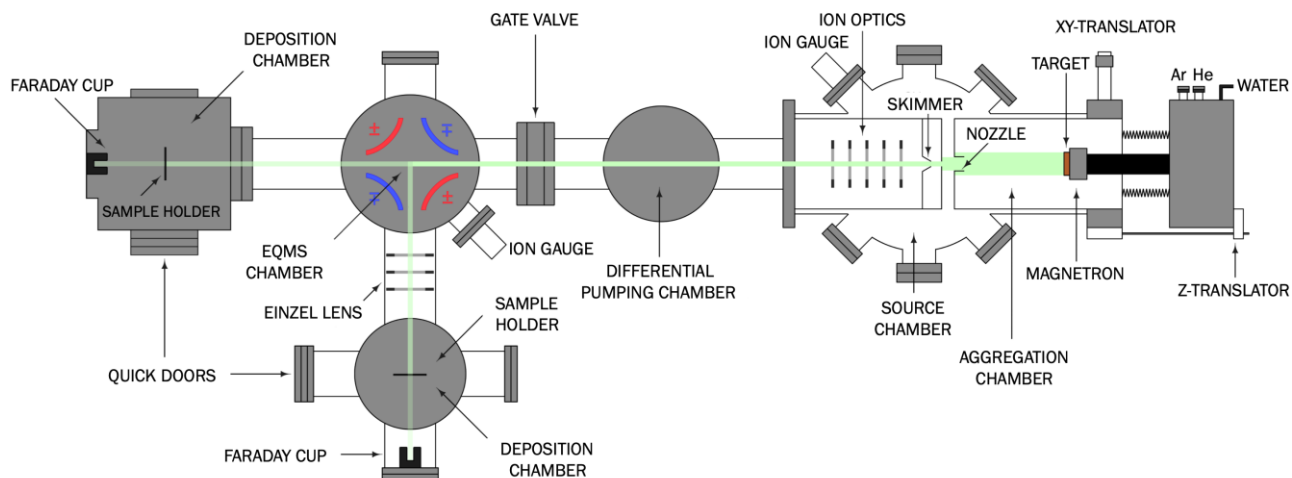
Figure 1. Schematic picture of MaSCA.

Figure 2. AFM images of silver NCs deposited on Si after mass filtering at (a) 200 V and (b) 1100 V. Examples of imperfections excluded from the analysis are shown by circles.
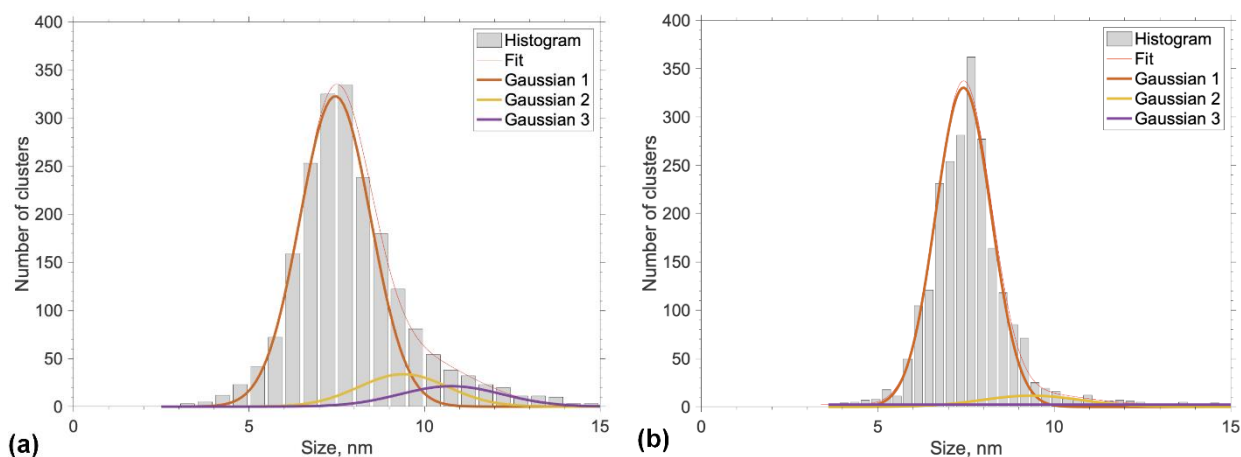
Figure 3. Histograms of height distribution for NCs deposited after filtering at 200 V selecting (a) anions and (b) cations. Histograms are fitted with Gaussian distributions for (1) singly-, (2) doubly- and (3) triply-charged particles.
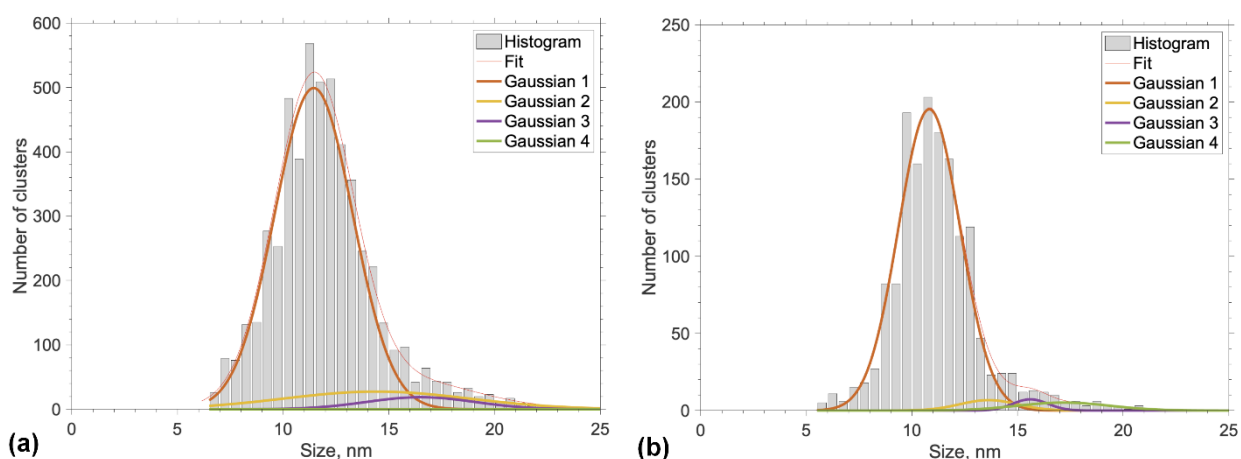

Figure 4. Histograms of height distribution for NCs deposited after filtering at 500 V selecting (a) anions and (b) cations. Histograms are fitted with Gaussian distributions for (1) singly-, (2) doubly-, (3) triply- and (4) quadruply-charged particles.
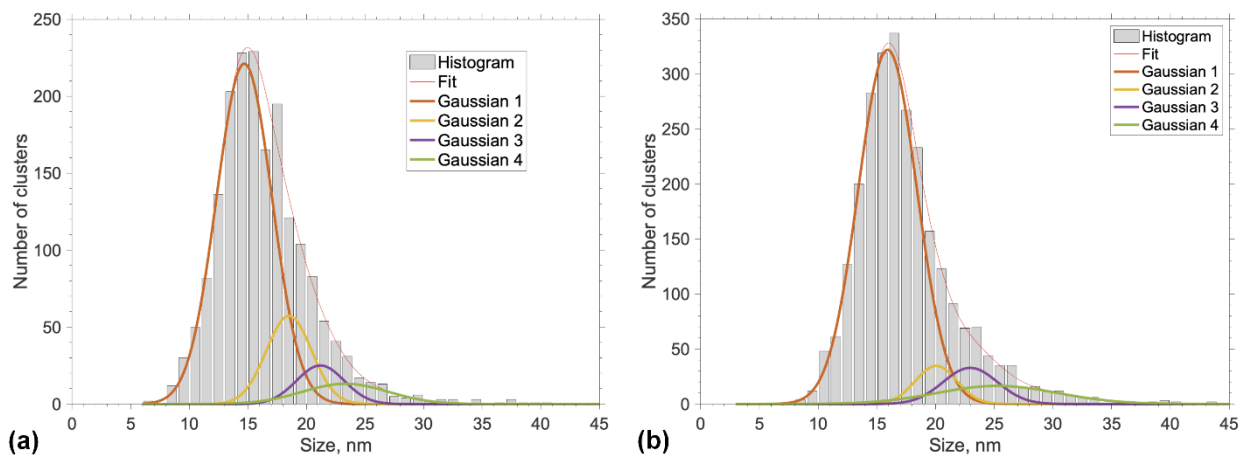
Figure 5. Histograms of height distribution for NCs deposited after filtering at 1100 V selecting (a) anions and (b) cations. Histograms are fitted with Gaussian distributions for (1) singly-, (2) doubly-, (3) triply- and (4) quadruply-charged particles.